FOREX Publication
Open Access | Rapid and quality publishing

International Journal of Electrical and Electronics Research (IJEER)
Research Article | Volume 13, Issue 4 | Pages 722-729 | e-ISSN: 2347-470X

Design and Simulation of a Standalone Solar Photovoltaic System for Water Pumping Using Induction Motor Drive

Abdulathim Alabdali[1*], and Asst. Prof. Dr. Abbas UĞURENVER[2]
[1]*MSc Student, Istanbul Aydin University, Turkey; afaysalalabdali@stu.aydin.edu.tr*
[2]*MSc Student, Istanbul Aydin University, Turkey; abbasugurenver@aydin.edu.tr*

***Correspondence:** *Abdulathim Alabdali*, Email: *afaysalalabdali@stu.aydin.edu.tr*

ABSTRACT- The rising demand for sustainable energy in off-grid regions has propelled the use of solar photovoltaic (PV) systems for water pumping, particularly for irrigation. This study investigates the design and simulation of a standalone PV-powered water pumping system employing a three-phase induction motor (IM) for remote applications. The research aims to optimize energy extraction and ensure system stability under varying solar irradiance. The methodology utilizes MATLAB/Simulink to model the system, integrating a Perturb and Observe (P&O) Maximum Power Point Tracking (MPPT) algorithm, a DC-DC boost converter, and a Voltage Source Inverter (VSI) to drive the IM. A standalone solar PV array rated at 5.84 kW was designed to drive a 4-kW induction motor water pump. Under simulated dynamic irradiance conditions, the motor load temporarily dropped to 2 kW, demonstrating the system's ability to maintain stable operation which reduces to 2.92 kW (half the rated capacity) during an irradiance drop from 1000 to 500 W/m² at $t=5$ seconds. The motor maintains a steady speed of 1430 rpm at a 4-kW load, with the P&O algorithm effectively adapting to dynamic conditions. The model acknowledges simplifications, noting that actual output may decrease by 10-15% due to temperature, inverter, and wiring losses. These findings affirm the system's potential for off-grid irrigation, though further refinements are recommended to address real-world inefficiencies and enhance reliability.

Keywords: Solar PV, Water pumping, Induction motor, MPPT, Irrigation.

ARTICLE INFORMATION
Author(s): Abdulathim Alabdali, and Abbas Ugurenver;
Received: 10/07/2025; **Accepted:** 22/09/2025; **Published:** 10/12/2025;
E- ISSN: 2347-470X;
Paper Id: IJEER 1007-08;
Citation: 10.37391/ijeer.130412
Webpage-link:
https://ijeer.forexjournal.co.in/archive/volume-13/ijeer-130412.html

Publisher's Note: FOREX Publication stays neutral with regard to jurisdictional claims in Published maps and institutional affiliations.

1. INTRODUCTION

The growing need for sustainable energy in remote, off-grid regions has underscored the importance of solar photovoltaic (PV) systems for applications like water pumping, particularly for irrigation. Traditional diesel-based systems are costly and environmentally harmful, making PV-driven induction motor (IM) pumps a promising alternative due to their durability and low maintenance. Previous research has explored MPPT algorithms and inverter designs [1], yet challenges remain in optimizing performance under fluctuating irradiance. "In this work, a 5.84 kW PV array is used as the primary power source. The system is designed to operate a 4-kW induction motor water pump under variable irradiance conditions. The system architecture adopted in this work follows previously published designs of standalone PV water pumping systems using induction motor drives [Singh et al., 2018; …]. Therefore, the contribution of this paper does not lie in proposing a new topology. Instead, the novelty of this study is in combining the conventional Perturb & Observe (P&O) MPPT algorithm with a scalar V/f control strategy and validating their performance comprehensively under various simulated solar irradiance conditions. This work further provides a step-by-step design and simulation approach that can serve as a practical guideline for engineers and researchers. The work aims to validate the system's stability and efficiency through simulation, addressing gaps in existing designs by integrating a P&O MPPT algorithm and a two-stage power conversion system. Key findings indicate robust operation with a stable DC link voltage, offering a viable solution for sustainable irrigation while highlighting areas for future improvement [2,3]

2. LITERATURE REVIEW

Solar PV technology has evolved significantly, with efficiencies rising from 5-6% to 15-20% in recent years, making it a viable alternative to conventional energy sources [10]. While grid-connected PV systems are common in urban areas, offering excess power to the grid, they rely on stable infrastructure, limiting their use in remote areas [11][12]. Standalone PV systems are preferred for off-grid irrigation but face challenges such as intermittency and energy storage needs [13][14]. In agriculture, PV pumping systems have gained traction, especially in developing countries where farming is widespread [15]. Early systems used DC motors, but induction motors. countries where farming is widespread [15]. Early systems used DC motors, but induction motors were adopted due to their robustness and lower maintenance needs [16]. Singh et al. [17] proposed a PV system for a 2.2kW motor using Incremental

FOREX Publication
Open Access | Rapid and quality publishing
International Journal of Electrical and Electronics Research (IJEER)
Research Article | Volume 13, Issue 4 | Pages 722-729 | e-ISSN: 2347-470X

Conductance (INC) MPPT, but its complexity led to a shift towards simpler algorithms like P&O [18]. A system demonstrated in [19] faced DC link voltage instability under low irradiance. In countries like India and Sub-Saharan Africa, solar PV systems for irrigation are growing. India's PM-KUSUM scheme promotes solar pumps, replacing diesel-based systems with PV-powered induction motors [20]. These systems, however, often require grid support or batteries, increasing costs. Standalone systems using centrifugal pumps are more efficient but require robust MPPT and motor control to handle irradiance variations [21]. The proposed design simplifies this with P&O MPPT, achieving over 95% efficiency, and enhances dynamic performance with a speed feedforward term, offering a solution for off-grid irrigation.

This paper is structured as follows: *Section 2* outlines the system design, *Section 3* details the P&O MPPT and control schemes, *Section 4* presents simulation results, *Section 5* compares findings with existing systems, and *Section 6* concludes with future research directions.

3. SYSTEM ARCHITECTURE AND DESIGN

The standalone solar PV water pumping system is designed to deliver power to a 4 kW IM that drives a centrifugal pump for irrigation in off-grid areas. The system employs a two-stage architecture consisting of a DC-DC boost converter and a VSI, enabling effective decoupling between the PV generation and motor load. PV array, boost converter, inverter, and the IM-driven pump. The PV array is sized to exceed the motor power requirement to account for conversion inefficiencies and dynamic irradiance. Control loops are implemented to regulate the DC-link.

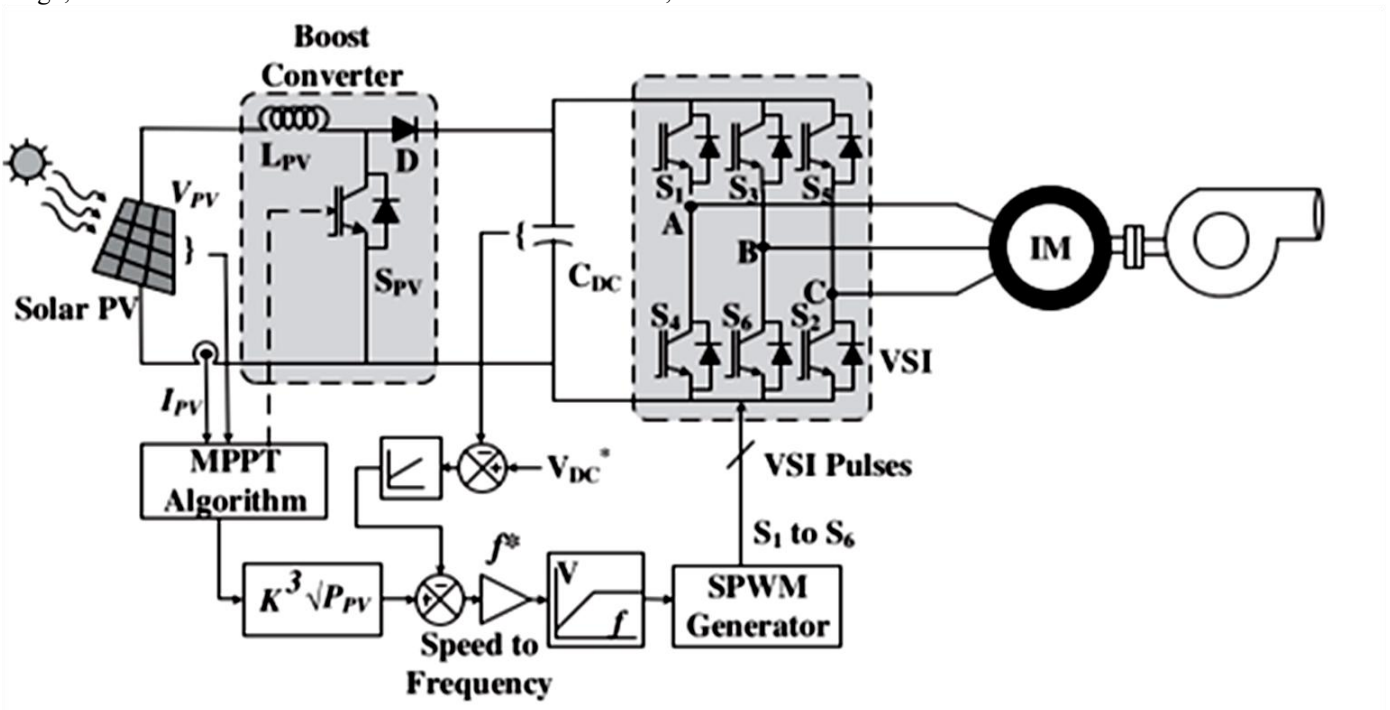

Figure 1. SLD of the proposed PV system [17]

Table 1. PV array cell and module parameters used in the system design

Parameter	Value
Module Type	User-defined Mono-Si
Rated Power (P_{mp})	150 W
Voltage at MPP (Vmp)	33.9 V
Current at MPP (Imp)	6.63 A
Open-Circuit Voltage (Voc)	42.1 V
Short-Circuit Current (Isc)	7.1 A
Number of Series Modules (Ns)	13
Number of Parallel Strings (Np)	2
Total Array Power	5.84 kW
Array MPP Voltage	440.7 V
Array MPP Current	13.26 A

3.1. PV Array Design

The The PV array was designed to meet the power demand of the induction motor-driven water pump. The rated capacity of the pump is 4-kW, and to ensure reliable operation under varying

FOREX Publication
Open Access | Rapid and quality publishing
International Journal of Electrical and Electronics Research (IJEER)
Research Article | Volume 13, Issue 4 | Pages 722-729 | e-ISSN: 2347-470X

irradiance conditions, a PV array of 5.84 kW was selected. Based on these calculations, the array configuration was finalized to supply the required DC link voltage and rated power. The design parameters of the PV array are summarized in *table 1* The design was carried out based on the following considerations:

- The motor requires a stable DC bus voltage of approximately 650V, which determines the series configuration of PV modules.
- The total required PV power capacity was determined to be greater than the motor's rated load to compensate for real-world losses (approximately 10–15%).
- Manufacturer datasheet values for VmpV_{mp}Vmp and ImpI_{mp}Imp were used to calculate the number of modules in series (NsN_sNs) and parallel (NpN_pNp) using:

$$P_{mp} = (V_{mp} * I_{mp}) \times (N_s * N_p) \quad (1)$$

$$P_{mp} = 5.84\ kw$$

where P_{mp} is the peak power, I_{mp} in Amper (A) and V_{mp} in voltage (V) are the current and voltage at maximum power point (MPP) of a single module, and N_p,N_s are the number of modules in parallel and series, respectively. The PV array is sized based on module ratings (V_{mp} =33.9 V, I_{mp} =6.63 a configuration of N_s=13, V_{mp}=2 This ensures the array operates efficiently near the inverter's required DC link voltage, enabling full motor load operation, as shown in *figure 1*. The electrical characteristics of the selected solar module and PV array configuration are summarized in *table 1*, which guides the sizing of the DC-DC converter, inverter input, and control algorithms under standard test conditions [23].

3.2. Boost Converter Design

The boost converter serves to elevate the PV array output voltage to a regulated DC-link voltage suitable for inverter operation. For the selected PV configuration of 13 modules in series (with V_{mp}=33.9 V), the array's maximum power point voltage is approximately:

$$V_{mp-array} = (N_s * V_{mp}) = 440.7\ V$$

To ensure sufficient headroom for the inverter, the DC link voltage is regulated at V_{dc}=650 V. The required duty cycle D of the boost converter is calculated using the standard boost equation:

$$D = \frac{V_{dc}-V_{mp}}{V_{dc}} = \frac{650-440}{650} = 0.321 \quad (2)$$

To size the boost inductor L_m, the peak-to-peak ripple current ΔI_1 is taken as 20% of the total array MPP current (I_{mp_total} =13.26 A). The inductor value is computed as:

$$L_m = \frac{V_{mp} \times D}{\Delta I_1 \times f_s} = 0.053mH$$

Where $V_{mp} = 440.7v$ and $D = 0.321$, $\Delta I_1 = 2.652\ A$, $and\ f_s = 10\ KHZ$ as *fs* is the switching frequency and ΔI_1 is ripple current [24].

3.3. DC Link Voltage and Capacitor Selection

The DC link voltage V_{dc} for the VSI is selected based on the required line-to-line output voltage of the three-phase induction motor. The relationship between the DC voltage and AC line voltage is given by:

$$m \times \frac{V_{dc}}{\sqrt{2}} = \frac{V_{LL}}{\sqrt{3}} = \frac{400}{\sqrt{3}} \quad (3)$$

where m is the modulation index (typically $m = 0.83$), and V_{LL} is the RMS line voltage of the motor. Substituting $V_{LL} = 380\ v$ yields:

$$V_{dc-LINK} = \frac{\sqrt{2}\times 380}{\sqrt{3}} = 465\ V$$

To provide sufficient headroom for voltage regulation and control dynamics, a higher DC link voltage is selected specifically, $V_{dcref} = 650\ V$. This ensures uninterrupted operation of the VSI, the DC link capacitor C_{dc} is sized using the energy balance method:

$$\frac{1}{2}C_{dc}[V_{dc1}^{*2} - V_{dc1}^{2}] = 3 \propto V_{phase}I_{phase}t \quad (4)$$

Where $\propto$ is over load factor, V_{phase} &I_{phase} are motor phase voltage and current, V_{dc1}^{*2} minimum accepting link voltage Assuming Vdc=0.95*650, t=5ms, and an estimated motor current of 8.9 A, the calculated capacitance is:

$$C_{dc} \approx 2000.6\ \mu f$$

This value ensures DC voltage stability during dynamic operating conditions, thereby supporting continuous and efficient power delivery to the motor [26].

3.4. Voltage Source Inverter (VSI) Design

VSI acts as the interface between the regulated DC link and the IM, converting the DC voltage into a variable frequency and amplitude AC supply. A standard three-phase, two-level VSI topology is used, which enables PWM control to synthesize sinusoidal output waveforms. The inverter output voltage is determined by the DC link voltage *Vdc* and the modulation index *m*. The relationship between the peak phase $V_{phase-peak}$ and the DC link is given by

$$V_{phase-peak} = m \times \frac{V_{dc}}{2} = 0.83 * \frac{650}{2} = 269.75\ V$$

For sinusoidal PWM with m=1, and a DC link voltage of Vdc=650 The corresponding RMS line-to-line voltage is given by $V_{LL} = \sqrt{3} \times \frac{V_{phase-peak}}{\sqrt{2}} \approx 380$ V This matches the motor's rated input, ensuring proper magnetization and torque production. The VSI operates at a switching frequency of 10 kHz to balance dynamic response and switching losses. To minimize harmonic distortion, a sinusoidal PWM technique is applied with symmetrical carrier waveforms. where output voltage and

FOREX Publication
Open Access | Rapid and quality publishing
International Journal of Electrical and Electronics Research (IJEER)
Research Article | Volume 13, Issue 4 | Pages 722-729 | e-ISSN: 2347-470X

frequency are adjusted proportionally to maintain a constant magnetic flux in the motor core V/F =Constance.

3.5. Induction Motor Design

IM rated at 4 kW and 380 V is selected to drive the centrifugal pump. Induction motors are preferred in such applications due to their simple construction, ruggedness, low cost, and compatibility with (V/f) scalar control [27]. The motor operates at a nominal speed of 1430 rpm, corresponding to a synchronous speed of 1500 rpm with a slip of approximately 4.7%. The motor's steady-state torque is defined by *equation (4)*.

$$T_L = K_{pump} \times \omega_r^2 \quad (5)$$

3.6. Centrifugal Pump Design

The motor is mechanically coupled to a centrifugal water pump. The pump's hydraulic characteristics and the motor's torque-speed characteristics determine the overall system's water delivery performance. The centrifugal pump follows the affinity laws where torque $T \propto \omega_r^2$ and power $P \propto \omega_r^3$. The pump constant K is defined based on *equation (5)*.

$$K_{pump} = \frac{T_L}{\omega_r^2} = 1.19 \times 10^{-3} N.m\,/(rad/s)^2 \quad (6)$$

where TL is the load toque of water pump, which is equal to the torque offered by an induction motor under steady-state operation and ωr is the rotational speed of the rotor in rad/s as rated torque and speer are 26.69 Nm and 1430 rpm, respectively [27].

4. CONTROL SCHEME

The induction motor is driven using a scalar V/f control strategy that maintains a constant voltage-to-frequency ratio to ensure stable torque and preserve magnetic flux. This open-loop method is computationally efficient and suitable for low-dynamic applications like water pumping. To enhance voltage stability under variable irradiance, the control includes a feedforward term where the reference speed is estimated from PV power using *equation (6);*

$$\omega^* = K_{pump} \times P_{pv}^{\frac{1}{3}} \quad (7)$$

where K is the feedforward constant derived from the pump's torque-speed profile. This value is adjusted using a Proportional-Integral (PI) controller that regulates the DC link voltage The controller compensates for power mismatches by modulating the reference frequency [29] based on *equation (7)* to *(9)*.

$$V_{dcr}(n) = V_{dc}^* - V_{dc}(n) \quad (8)$$

$$\omega_{dcr}(n) = \omega_{dcr}(n-1) + K_p * [V_{dcr}(n) - V_{dcr}(n-1)] + K_i * V_{dcr}(n) \quad (9)$$

$$f^* = \frac{1}{2\pi} * (\omega^* - \omega_{dcr}) \quad (10)$$

This hybrid approach, combining feedforward speed estimation and voltage feedback regulation, enhances dynamic stability during irradiance variations and reduces dependency on current or speed sensors as cleared in *figure 2*.

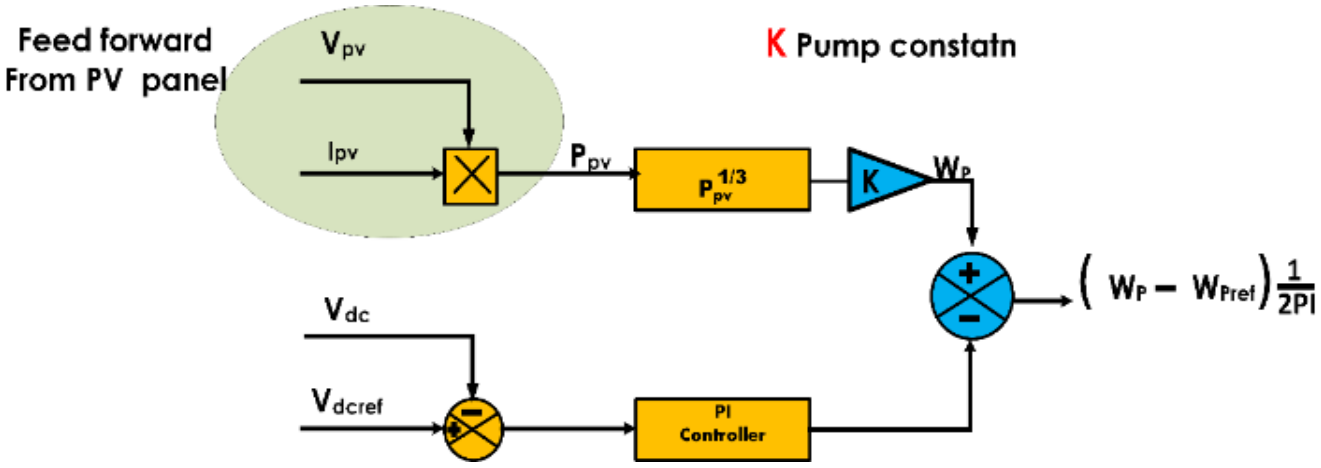

Figure 2. Control scheme for reference speed generation using PV power feedforward and DC link PI control

4.1. Perturb and Observe MPPT

The proposed system uses the P&O algorithm to track the MPP of the PV array under dynamic environmental conditions. The algorithm perturbs the operating voltage and observes the change in power, as described by *equations (10)* and *(11)*.

$$\Delta P = P(k) - P(k-1) \quad (11)$$

$$v(k+1) = \begin{cases} v(k) + \Delta v \; if \; \Delta P > 0 \\ v(k) + \Delta v \; otherwise \end{cases} \quad (12)$$

where P(k) and P(k−1) are the current and previous power outputs. If ΔP> 0, the perturbation continues in the same direction; otherwise, the direction is reversed. The voltage is updated as follows:

FOREX Publication
Open Access | Rapid and quality publishing
International Journal of Electrical and Electronics Research (IJEER)
Research Article | Volume 13, Issue 4 | Pages 722-729 | e-ISSN: 2347-470X

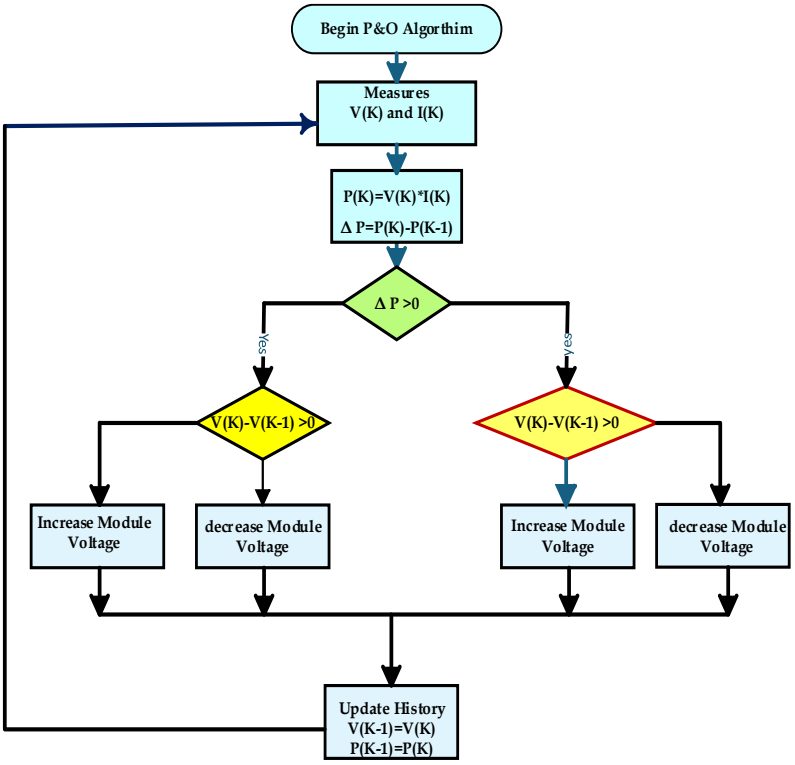

Figure 3. Flowchart illustrating the P&O MPPT algorithm for tracking the maximum power point in PV systems

5. SIMULATION RESULTS

The performance of the designed standalone solar PV water pumping system was evaluated through simulations conducted in MATLAB/Simulink, focusing on key aspects like MPPT efficiency, DC link voltage regulation, motor startup behaviour, and overall system stability under varying solar irradiance conditions. The simulation results validate the effectiveness of the proposed system configuration and control strategies.

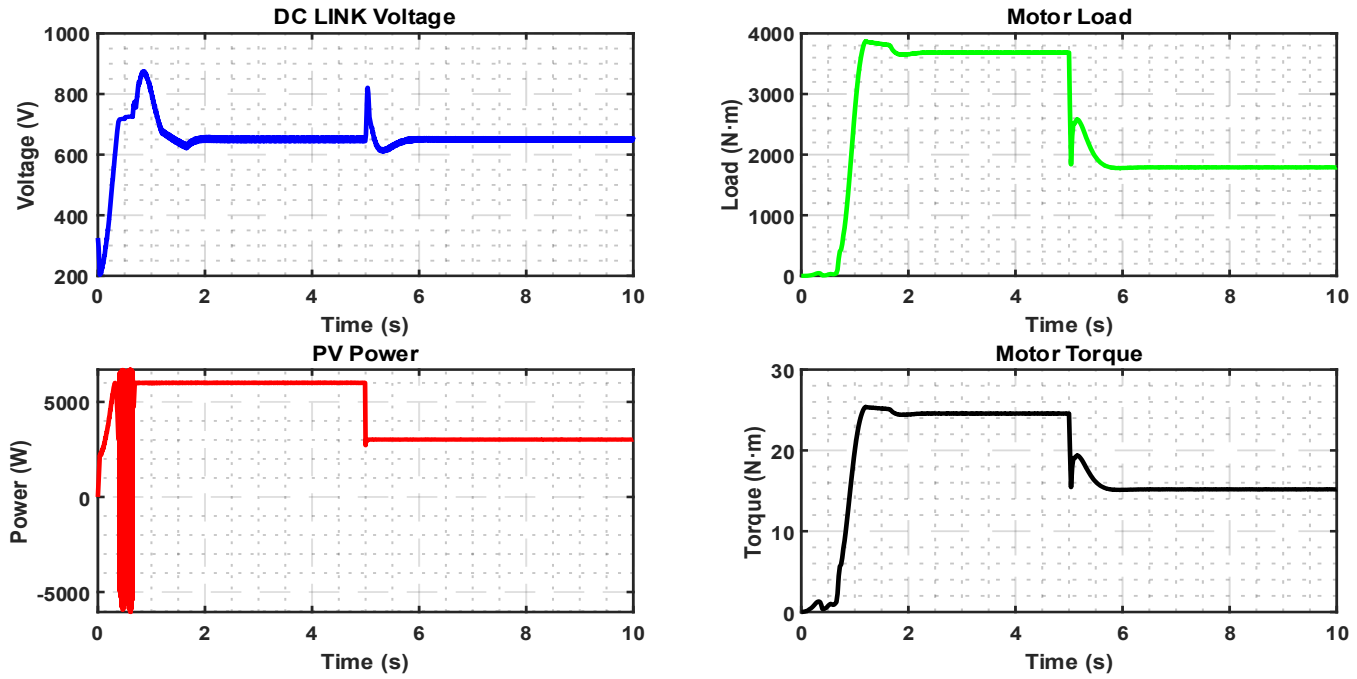

Figure 4. Motor load profile showing rated operation at 4 kW with a temporary drop to 2 kW under reduced irradiance conditions at t = 5s

FOREX Publication
Open Access | Rapid and quality publishing
International Journal of Electrical and Electronics Research (IJEER)
Research Article | Volume 13, Issue 4 | Pages 722-729 | e-ISSN: 2347-470X

The results shown in *figure 4* illustrate the proposed system performance for a sudden reduction from a value of 1000 W/m² to 500 W/m² at *t=5* seconds. Which reflects the behaviors of DC Link voltage which it affected by irradiance change and then rearrange its performance based on the response of the PI controller on other hand the PV power is reduced to its half of 3 kw with reduction in motor load of 2KW as a result notable decrease in the motor torque which ensures the performance of the used P&O against the sudden change in the irradiance, to evaluate the whole performance of the proposed system The simulation results showed in *figure 5* contain six cases of signal responses under irradiance of 1000 W/m². Simulation results show the DC link voltage *p*, which stabilizes at 650 V after fluctuating initially. The DC link capacitor starts with an initial value of 352 µF to ensure stability.

The PI controller adjusted its output to maintain the DC link voltage which reflects on the performance of the boost converter and the PV output power. The equivalent duty cycle is shown in *figure 6*, demonstrating the dynamic and effective nature of the P&O-based MPPT controller.

Then the PV power settles and achieves its nominal value of 5.84 kW, as can be seen in the PV power plot. The motor speed also achieves its nominal value of 1430 rpm at a rated load of 4 kW. The V/F control response mirrors the stator current behavior, which has a slight fluctuation during the starting time but afterwards settles at its nominal value. The system also creates rated steady-state torque, confirming the ability of the proposed model to guarantee performance specifications.

Figure 6 also provides the behavior of the P&O algorithm to adjust a duty cycle of approximately 0.321, which maintains the DC link voltage within an acceptable range for the VSI to supply the required voltage to the induction motor.

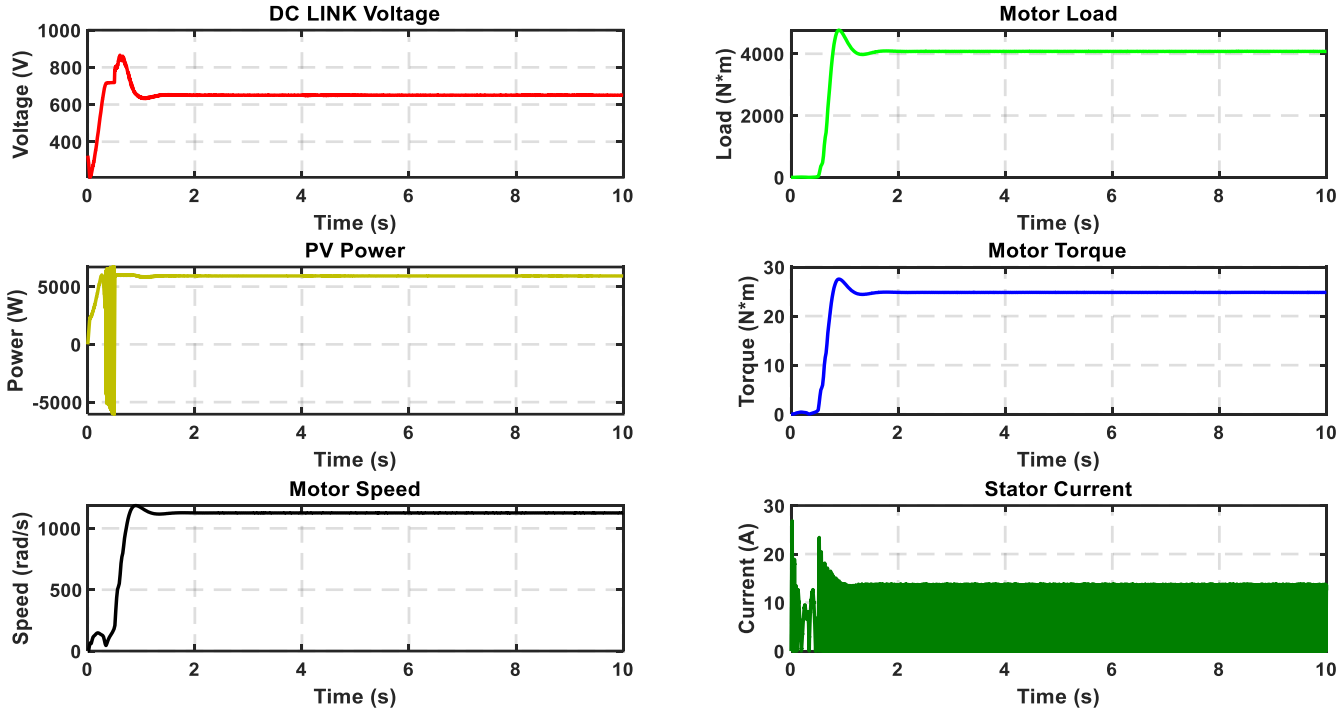

Figure 5. System response under 1000 W/m² irradiance with PI control maintaining a stable 650V DC link voltage

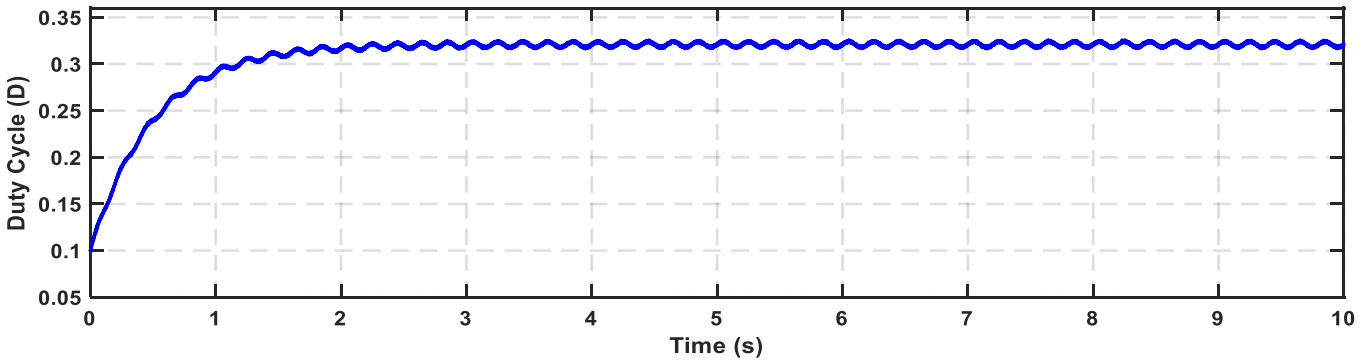

Figure 6. dynamic and effective performance of the P&O

FOREX Publication
Open Access | Rapid and quality publishing
International Journal of Electrical and Electronics Research (IJEER)
Research Article | Volume 13, Issue 4 | Pages 722-729 | e-ISSN: 2347-470X

5.1. Comparative Analysis

To further validate the effectiveness of the proposed system, a comparison with previously published methods was carried out. Table 2 summarizes the key performance indicators such as MPPT efficiency, DC link voltage regulation, and transient response under irradiance changes. It can be observed that the proposed P&O-based system achieves stable DC link operation and satisfactory MPPT efficiency, comparable to or slightly better than existing methods, while maintaining a simpler control structure and requiring fewer sensors.

Table 2. Comparative analysis of the proposed system and existing methods based on MPPT efficiency, DC link stability, transient response, and implementation complexity

Reference	MPPT Algorithm	Control Strategy	MPPT Efficiency	DC Link Voltage Stability	Transient Response	Sensors
Proposed System	P&O	Scalar V/f	~98%	Stable	<0.2s	Low, fewer
[17]	INC	V/f Control	~97%	Stable	~0.25s	Moderate
[19]	AI-based MPPT	BLDC Motor	~99%	Very stable	Fast (<0.1s)	requires sensors
[22]	Simple P&O	Six-step Inverter	~95%	Less stable	Slower	Very low complexity

6. LIMITATIONS AND PRACTICAL CONSIDERATIONS

The proposed design and simulation assume ideal PV module characteristics, converter switching without losses, and perfect motor operation. In real-world implementation, however, additional factors such as thermal effects, wiring resistance, inverter switching losses, and mechanical pump inefficiencies can reduce the overall system efficiency by approximately 10–15%. Furthermore, the study does not account for long-term degradation of PV modules or variability in water demand, which may influence system performance. These limitations should be carefully considered when scaling the design for field deployment.

7. CONCLUSION

The proposed 5.84 kW PV system successfully drives a 4-kW induction motor water pump, with the ability to sustain operation even under reduced irradiance where the dynamic load momentarily decreases to 2-kW. These issues primarily arise due to variations in solar power input, which can affect the system's performance, *i.e.*, motor starting, power stability, and torque control. However, application of the P&O MPPT algorithm and scalar V/f control greatly minimizes these effects, allowing efficient operation even against transient irradiance levels. While intrinsic challenges are faced in the operation of a 4-kW motor from dynamic solar resources, the system successfully offers stable DC link voltage regulation at 650V, thus establishing the reliable operation of the motor. The PI controller plays a major role in minimizing the impact of changes in irradiance so that a steady motor speed, load, and torque are maintained throughout. The functionality of the boost converter, while being temporarily interrupted during power dips, reflects the system's ability to cope under realistic scenarios. Future optimization of the response time of the system along with improvement in the efficiency of the system during low irradiance would be worthwhile enhancements. This can include looking into more sophisticated control techniques, i.e., model predictive control (MPC) or fuzzy controllers, to enhance the system's response to sudden changes in the availability of solar energy. Further, the inclusion of energy storage solutions will enhance system stability and maintain continuous power supply during low irradiance periods or nighttime, with off-grid reliability. It is important to note that the architecture itself is not new and is based on prior works. The contribution of this paper lies in the integration and detailed simulation of P&O MPPT with V/f control under dynamic irradiance conditions, highlighting its feasibility as a low-cost, practical solution. “Beyond the technical findings, the proposed system provides a low-cost, robust, and sustainable solution for off-grid irrigation. This is particularly relevant for rural communities in regions such as India and Sub-Saharan Africa, where access to reliable electricity is limited. By relying on solar energy and reducing the need for fuel-based pumps, the system has potential environmental and socio-economic benefits, including reduced carbon emissions and improved agricultural productivity.

REFERENCES

[1] Zahedi, A., 2006. Solar photovoltaic (PV) energy; latest developments in the building integrated and hybrid PV systems. Renewable energy, 31(5), pp.711-718.

[2] Sahu, B.K., 2015. A study on global solar PV energy developments and policies with special focus on the top ten solar PV power producing countries. Renewable and Sustainable Energy Reviews, 43, pp.621-634.

[3] Narendra, A., Naik, N.V., Panda, A.K. and Tiwary, N., 2020. A comprehensive review of PV driven electrical motors. Solar energy, 195, pp.278-303.

[4] Anand, R. and Saravanan, S., 2016. Solar PV system for energy Conservation incorporating an MPPT based on computational intelligent techniques supplying brushless DC motor drive. Circuits and Systems, 7(08), p.1635.

[5] Suetake, M., da Silva, I.N. and Goedtel, A., 2011. V/f Speed Control. IEEE Transactions on Industrial Electronics, 58(3).

FOREX Publication
Open Access | Rapid and quality publishing
International Journal of Electrical and Electronics Research (IJEER)
Research Article | Volume 13, Issue 4 | Pages 722-729 | e-ISSN: 2347-470X

[6] Wasynezuk, O., 2007. Dynamic behavior of a class of photovoltaic power systems. IEEE transactions on power apparatus and systems, (9), pp.3031-3037.

[7] Laudani, A., Lozito, G.M. and Riganti Fulginei, F., 2021. Irradiance sensing through PV devices: a sensitivity analysis. Sensors, 21(13), p.4264.

[8] Bhagyashree, S.M. and Khule, S.S., 2017, July. Design of solar water pumping system with FCMA soft starter. In 2017 International Conference on Computing Methodologies and Communication (ICCMC) (pp. 951-954), IEEE.

[9] Zhao, Z., Yang, P., Wang, Y., Xu, Z. and Guerrero, J.M., 2017. Dynamic characteristics analysis and stabilization of PV-based multiple microgrid clusters. IEEE Transactions on Smart grid, 10(1), pp.805-818.

[10] Stritih, U., 2016. Increasing the efficiency of PV panel with the use of PCM. Renewable Energy, 97, pp.671-679.

[11] Kouro, S., Leon, J.I., Vinnikov, D. and Franquelo, L.G., 2015. Grid-connected photovoltaic systems: An overview of recent research and emerging PV converter technology. IEEE Industrial Electronics Magazine, 9(1), pp.47-61.

[12] Srisaen, N. and Sangswang, A., 2006, December. Effects of PV grid-connected system location on a distribution system. In APCCAS 2006-2006 IEEE Asia Pacific conference on circuits and systems (pp. 852-855), IEEE.

[13] Hansen, A.D., Sørensen, P.E., Hansen, L.H. and Bindner, H.W., 2001. Models for a stand-alone PV system.

[14] Egido, M. and Lorenzo, E., 1992. The sizing of standalone PV-system: A review and a proposed new method. Solar energy materials and solar cells, 26(1-2), pp.51-69.

[15] Campana, P.E., Li, H. and Yan, J., 2013. Dynamic modelling of a PV pumping system with special consideration on water demand. Applied energy, 112, pp.635-645.

[16] Mokeddem, A., Midoun, A., Ziani, N., Kadri, D. and Hiadsi, S., 2007, December. Test and analysis of a photovoltaic DC-motor pumping system. In 2007 ICTON Mediterranean Winter Conference (pp. 1-7), IEEE.

[17] Singh, B., Sharma, U. and Kumar, S., 2018. Standalone photovoltaic water pumping system using induction motor drive with reduced sensors. IEEE transactions on industry applications, 54(4), pp.3645-3655.

[8] Tezer, T., Yaman, R. and Yaman, G., 2017. Evaluation of approaches used for optimization of stand-alone hybrid renewable energy systems. Renewable and Sustainable Energy Reviews, 73, pp.840-853.

[19] Anand, R., & Saravanan, S. (2016). Solar PV system for energy Conservation incorporating an MPPT based on computational intelligent techniques supplying brushless DC motor drive. Circuits and Systems, 7(08), 1635.

[20] Bhati, K., 2022. A ray of self-dependency by the energy of sun for the Indian farmers through PM KUSUM scheme. Just Agriculture, 2(11), pp.1-7.

[21] Alshahrani, A., Omer, S., Su, Y., Mohamed, E. and Alotaibi, S., 2019. The technical challenges facing the integration of small-scale and large-scale PV systems into the grid: A critical review. Electronics, 8(12), p.1443.

[22] Hyder, F., Sudhakar, K. and Mamat, R., 2018. Solar PV tree design: A review. Renewable and Sustainable Energy Reviews, 82, pp.1079-1096.

[23] Hasaneen, B.M. and Mohammed, A.A.E., 2008, March. Design and simulation of DC/DC boost converter. In 2008 12th International Middle-East Power System Conference (pp. 335-340), IEEE.

[24] Hashim, N., Salam, Z., Johari, D. and Ismail, N.F.N., 2018. DC-DC boost converter design for fast and accurate MPPT algorithms in stand-alone photovoltaic system. International Journal of Power Electronics and Drive Systems, 9(3), p.1038.

[25] Hawsawi, M., Habbi, H.M.D., Alhawsawi, E., Yahya, M. and Zohdy, M.A., 2023. Conventional and switched capacitor boost converters for solar PV integration: Dynamic MPPT enhancement and performance evaluation. Designs, 7(5), p.114.

[26] Munoz-Garcia, A., Lipo, T.A. and Novotny, D.W., 2002. A new induction motor V/f control method capable of high-performance regulation at low speeds. IEEE transactions on Industry Applications, 34(4), pp.813-821.

[27] Lobanoff, V.S. and Ross, R.R., 2013. Centrifugal pumps: design and application. Elsevier.